COBEM 2023 27TH INTERNATIONAL CONGRESS OF MECHANICAL ENGINEERING

ABCM Brazilian Society of Mechanical Sciences and Engineering
27th ABCM International Congress of Mechanical Engineering
December 04-08, 2023, Florianópolis-SC, Brazil

COB-2023-1475

CLASSIFICATION OF FLOW PATTERNS IN AIR-WATER FLOWS USING CONFOCAL CHROMATIC MICROSCOPY

Fernando Neves Quintino
Cristiano Bigonha Tibiriçá
Heat Transfer Research Group, Department of Mechanical Engineering, São Carlos School of Engineering, University of São Paulo, São Carlos, Brazil
fernandonquintino@usp.br
bigonha@sc.usp.br

Abstract. *Two phase-flow has several applications, including but not limited to refrigeration or power generation. Several factor influences the flow, such as flow pattern, tube geometry, velocity, and other. One important parameter is the flow pattern, as it has a close relationship in the behavior of important parameters such as pressure drop, and phase dispositions. Flow patterns can be divided into two main categories: dispersed and separated flows. Despite its importance, this classification is subjective, as there is no consolidated objective method for classification. This paper proposes the use of a novel optical technique called chromatic confocal microscopy to classify flow patterns. It works measuring the wavelength of focal reflections happening in the interfaces (eg. glass-liquid or liquid-glass). As there is a significant difference in the liquid-gas interfaces in the flow patterns, the sensor output signal can be used for flow classification. Advantages of the technique are that it has a high measurement rate, is non-intrusive, and can measure distance, which can be used to measure liquid thickness and waves. Experiments were conducted in a air-water horizontal flow, in a 8 mm squared tube, using a confocal chromatic microscope to evaluate liquid thickness. Results point that the technique is adequate for intermittent flows.*

Keywords: *multiphase flow, flow patterns, air-water, confocal chromatic microscopy*

1. INTRODUCTION

Two-phase flows can be classified in different flow patterns, according to the topology of the flow. Those flow patterns are a function of the fluids, channel size and material, and operating conditions. Usually the patterns are identified visually using high-speed cameras, so there is always a degree of subjectivity involved. In an attempt to standardize the classification, Thome *et al.* (2013) proposed only five different patterns divided in two major categories - dispersed and separated flow. Dispersed flows includes bubbles and mist, while separated flows contains intermittent (plug and slug), stratified and annular. Visualization of each flow pattern can be found on (Triplett *et al.*, 1999; Chen *et al.*, 2006; Thome *et al.*, 2013). Associated with the classification are flow pattern maps, that can be either experimental or mechanistic. Some well-known experimental maps includes Mandhane *et al.* (1974) and Wambsganss *et al.* (1991), while Taitel and Dukler (1976) and Wojtan *et al.* (2005) are examples of mechanistic maps.

Due to the subjective nature of visual classification, new objective methods are desired to classify flow patterns. One strategy to do that, is using the shape of the signal response. Wambsganss *et al.* (1991) evaluated the root mean squared pressure drop signal along with the mass quality to find flow pattern transition. Revellin *et al.* (2006) proposed a method using the electrical response of lases and diodes to classify each pattern. One parameter that can be used directly for this objective classification is the liquid film thickness. It has a distinct temporal shape in each flow pattern, is useful to calculate the void fraction, and is also used in mechanistic models for heat transfer and pressure drop (Cioncolini and Thome, 2013). Tibiriçá *et al.* (2010) reviewed several techniques for liquid film assessments, and classified them in acoustic, electrical, optical and nucleonic. Techniques differ on precision, cost, applicability for various channel sizes and fluids. The authors highlight that the confocal chromatic microscopy is an interesting technique, much used in microbiology applications due to its precision, yet little explored in fluid mechanics. Berto *et al.* (2021) used this technique to measure liquid film thickness as low as 25 µm during R245fa condensation in a vertical 3.38 mm tube. Other studies includes Seo *et al.* (2021) which measured the liquid film thickness in a heated annular channel and Zaitsev *et al.* (2022) which adapted the technique to measure ultra-thin films.

The objective of this study is to evaluate the changes in the probability density function (PDF) of the liquid film thickness measured using chromatic confocal microscopy. Experiments were conducted using air-water horizontal flow in a 8 mm squared aluminum channel.

2. METHODOLOGY

Figure 1 shows the schematic of the experimental rig used. It has a line of compressed air, one of liquid, that mixes at the beginning of the test section, exiting the test section in liquid separator, closing the circuit. The gas flow is measured using a orifice plate, while the liquid flow is measure using a turbine flow meter. Both liquid and gas flow sensor were calibrated and have uncertainty maximum uncertainty of ±3 %. Liquid and gas flows are adjusted using needle valves. The test section consists of a squared channel made of aluminum, which 150 cm length. A visualization section made of borosilicate 30 cm length, 8 mm internal side and 0.9 mm nominal thickness was installed 90 cm from test section beginning. The chromatic confocal microscope, used to measure the liquid film thickness, consists of a controller and a probe, united by a fiber optic cable. The controller is isolated, while the probe is place below the test section, at about 100 cm from the start of the test section. The controller unit is a Micro-Epsilon Confocal DT IFC2451 MP with an IFS2405-10 probe. It has a measuring range of 10 mm, uncertainty of ±20 µm, and the minimum thickness it can measure is 500 µm considering a flat glass with refractive index of 1.5 and maximum tilt angle of ±17°.

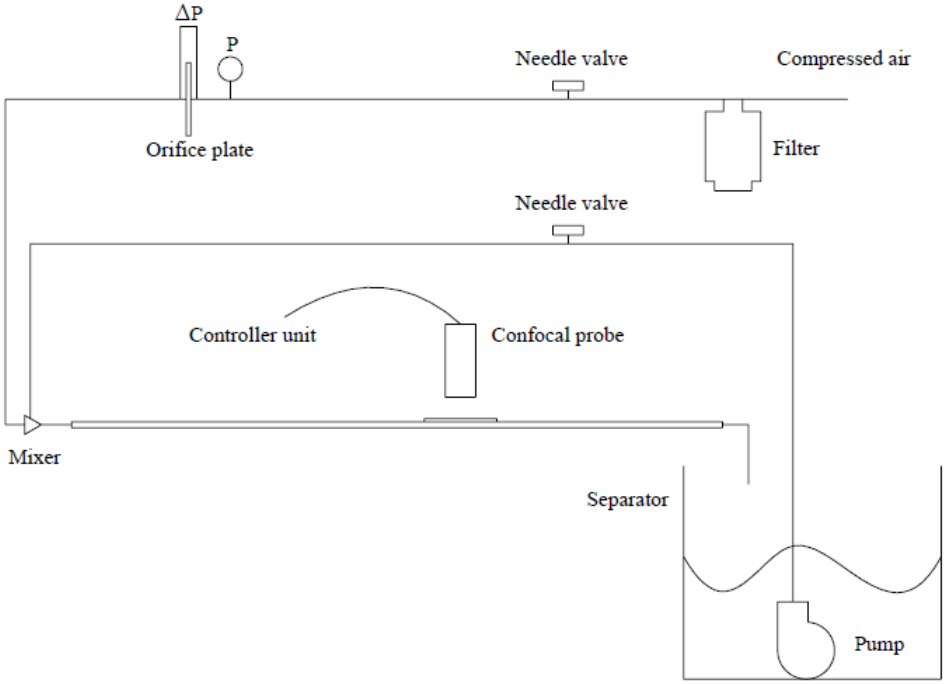

Figure 1. Experimental rig schematic.

2.1 Measurement principle

Figure 2 shows a schematic of the chromatic confocal measurement principle. It works as a light source in the controller emits a white light, that goes to the probe via fiber optic cable. Then, the light is dispersed in the various wavelength through a set of lens, resulting in a conic shape with all wavelengths. All of them are focused on the same center point, varying only the height coordinate. When in contact with a surface, there is a focal reflection, that goes through a pinhole, and is evaluated in a spectrometer. The wavelength of the focal reflection corresponds to a distance, via factory calibration. When used on transparent mediums, part of the part refracts. This can be used to measure several distances, as each change in medium corresponds to a focal reflection. The thickness can then be evaluated using the difference in distances. One important aspect to take care is to make a refractive index correction, as the light changes direction in each medium change. This can be done automatically through the software of the sensor.

2.2 Experiments

The confocal chromatic microscopy is specially adequate for measuring liquid thickness in separated flows. One way to identify flow patterns is evaluating the probability density function of the temporal output of the sensor. In stratified flows, it is expected to have a peak value on the mean height, with small oscillations corresponding to waves. In intermittent flows, it is expected to find two distinct pictures, one corresponding to when there is only liquid flowing, and the other for the liquid film between the channel and the gas bubble. Annular flows, despite not being the object of this study, is similar to the stratified flow, but with a much lower liquid film thickness.

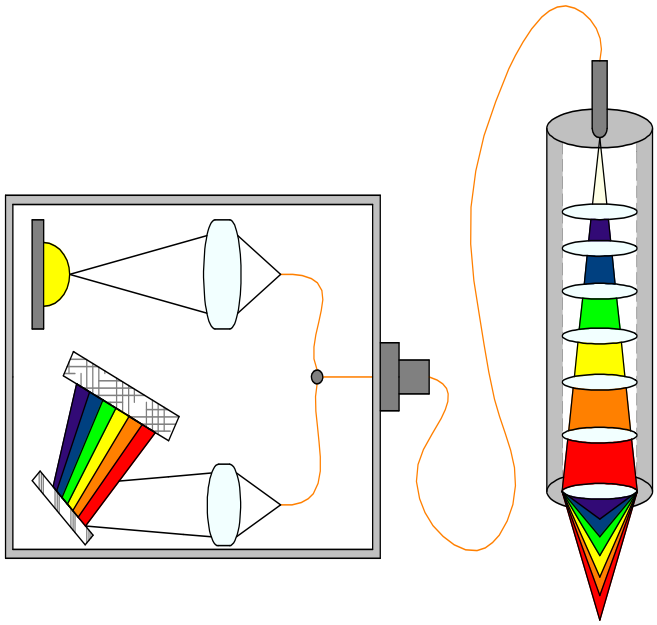

Figure 2. Chromatic confocal microscope schematic.

For this paper experiments were conducted in intermittent flow. Figure 3 shows the experimental conditions in a flow pattern developed by (Coleman and Garimella, 1999) using air-water flow in a 5.5 mm squared channel. Two different liquid superficial velocities (j_l) were evaluated, 0.30 m/s and 0.43 m/s, with four different gas superficial velocities (j_g) in each case.

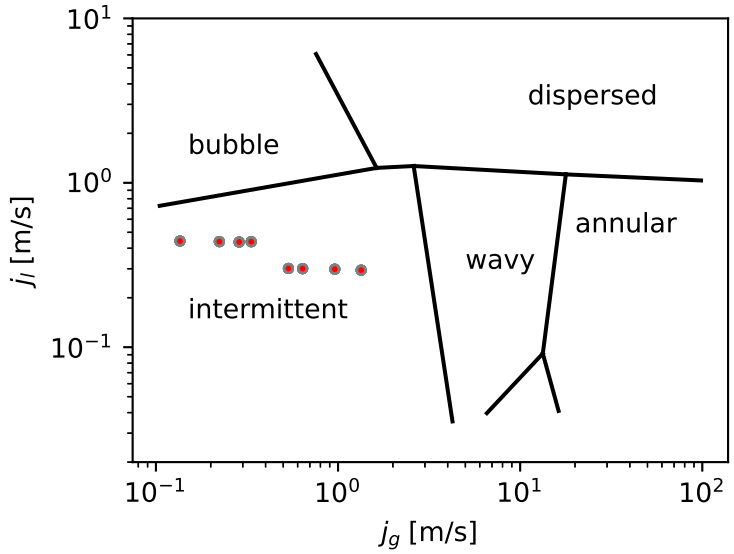

Figure 3. Experimental conditions shown in Mandhane *et al.* (1974) flow pattern map.

2.3 Data reduction

The data obtained by the confocal microscope contains three columns: time (t[s]), glass thickness (t_1[mm]), liquid thickness (t_2[mm]). When the sensor is not able to measure one of the values (usually when there is little distinction in the thickness or a high curvature in the piston), the output is −10, which was later substituted by a null. In some cases, the sensor do not distinguish the glass from the liquid, so t_1 becomes an outlier. In those cases the data is removed to avoid cases that where the sensor measure the glass and liquid film thickness combined. Figure 4 shows the glass thickness value measured in four different experimental conditions. For higher superficial velocities more data is removed, however the mean glass thickness remains close to 0.93 mm. After this first step, outlier liquid thickness were removed. Despite the

tube side being 8 mm, all cases below 8.5 mm were selected, to incorporate the experimental uncertainty. Finally, the data was smoothed using the rolling average of eight periods.

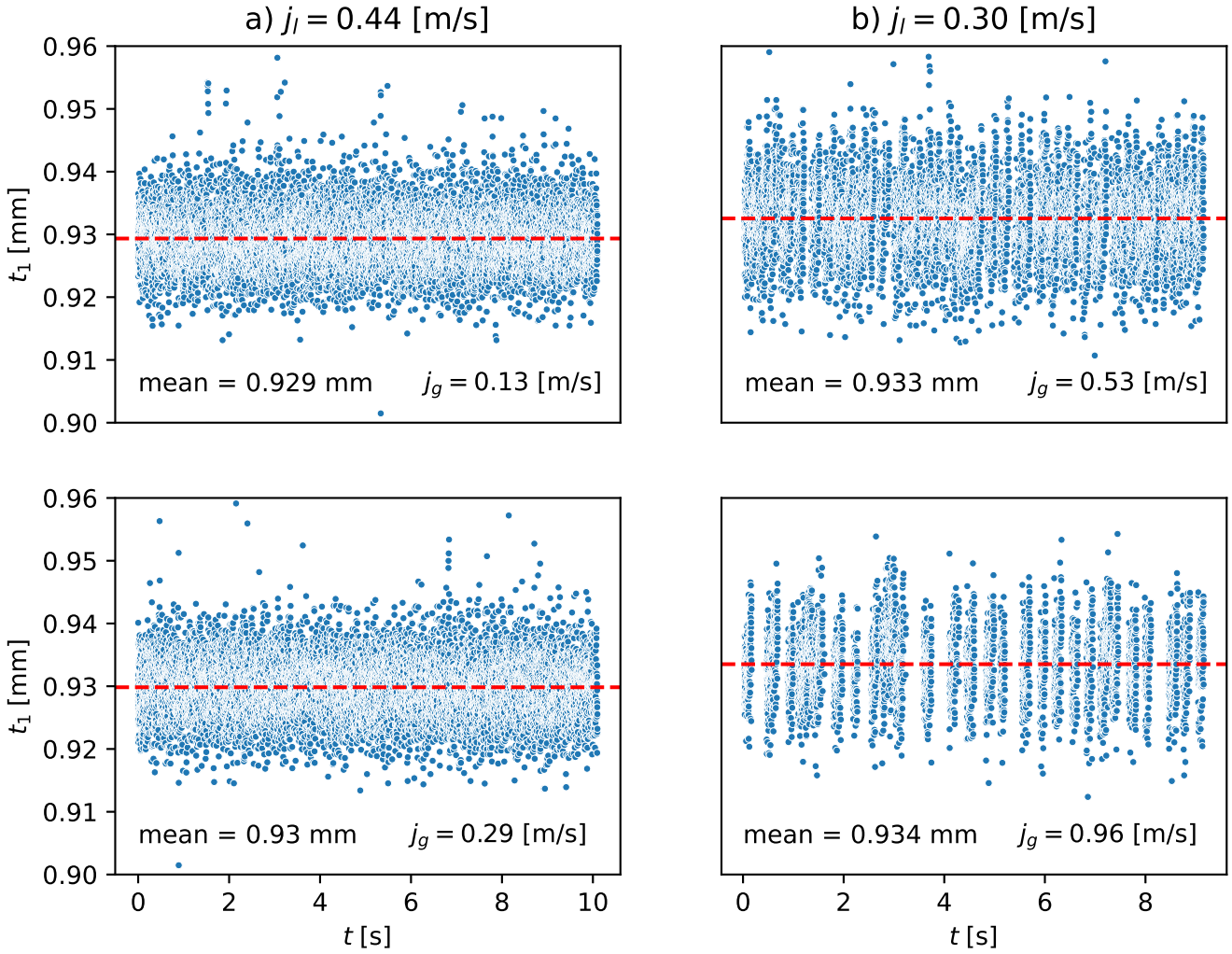

Figure 4. Glass thickness measurements.

3. RESULTS

Figure 5 shows the flow profile for all experimental conditions. The line represents the liquid thickness, so everything above can be thought as gas bubble. The plots on the left shows that the plug frequency increases with increased gas velocity, while plots in the right shows a different behavior. This happens because those operational conditions are closer to wavy flow, so the bubbles coalesce making gas bubbles with higher length.

Figure 6 depicts the probability density function for the operational conditions. In both liquid superficial velocities there are two peaks, which is expected in intermittent flows; one with a low liquid film thickness, and the other the passing of the liquid plugs. The plots on the left have a higher density on the 8 mm, which is the liquid plug, while the ones on the right have a similar behavior but the highest density is in the peak with lower thickness. This suggests that the probability density function can be used as an indicative of intermittent flow pattern, and closeness to transition.

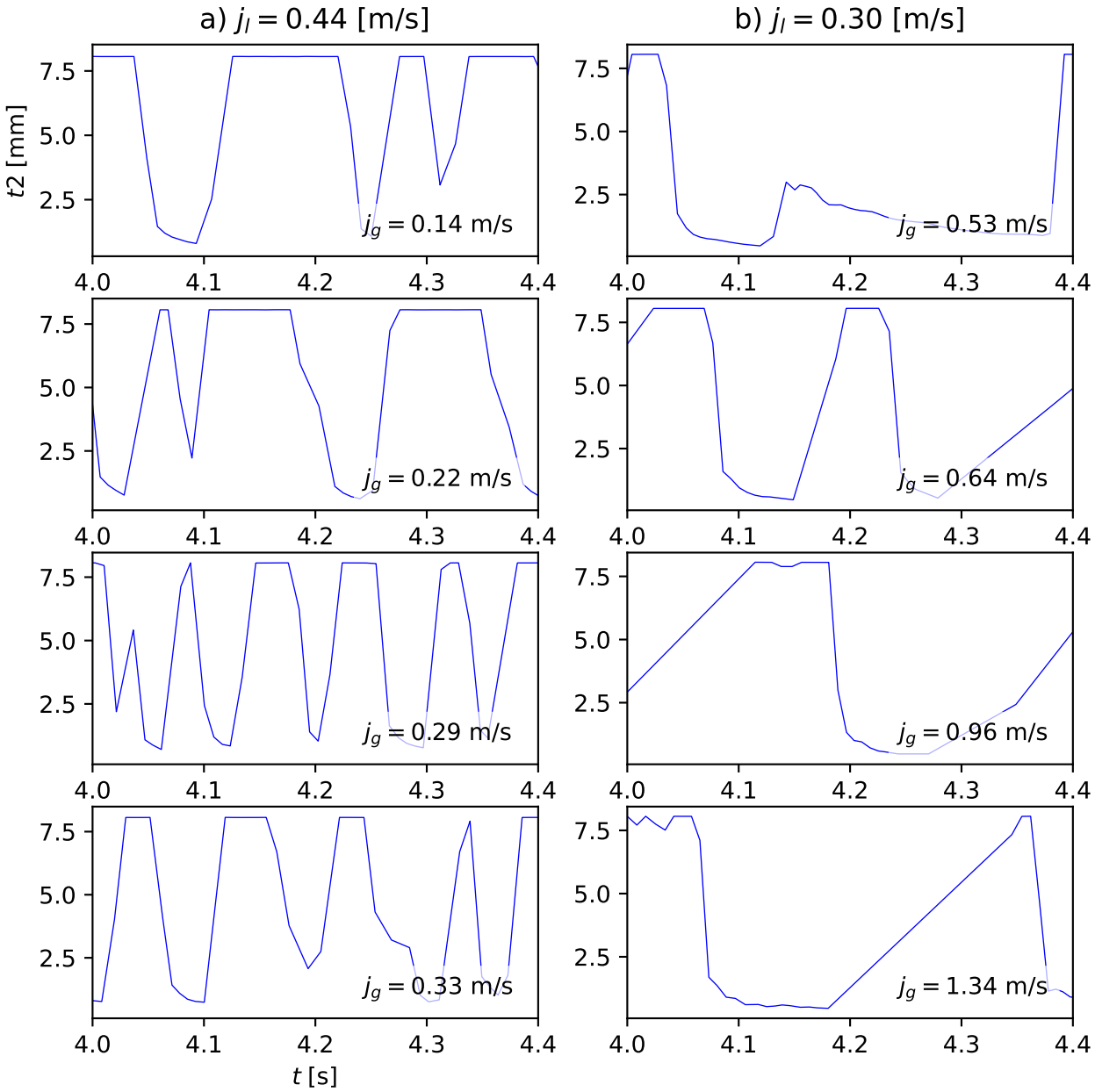

Figure 5. Liquid film thickness profile for different superficial velocities.

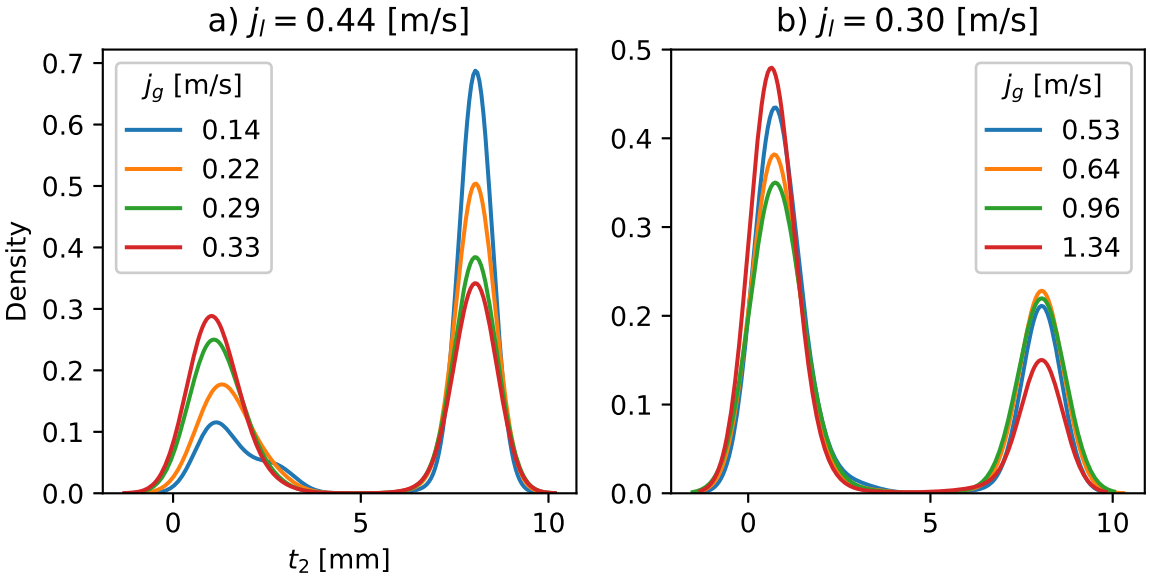

Figure 6. Probability density function of the liquid film thickness profile.

Figure 7 shows the mean film thickness. To calculate it, only cases where the liquid thickness was below 7 mm were included, as to exclude the liquid plugs. It can be seem that the film thickness reduces when the gas superficial velocity increases, which is expected, as the gas bubbles becomes bigger. In the case of the liquid superficial velocity 0.30 m/s, there is a change in the pattern, which is credited to the uncertainty of the experiment.

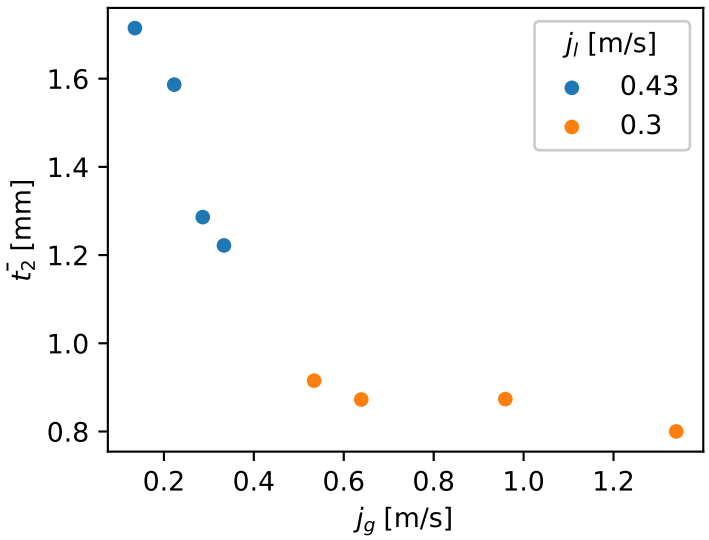

Figure 7. Time averaged liquid film thickness.

4. CONCLUSIONS

The response of the chromatic confocal microscope was evaluated in two sets of intermittent flows. Measurements of the liquid film thickness showed that with increasing gas valocity there is a corresponding reduction in the film thickness. The probability density function for those conditions have two peaks, one corresponding to the liquid film below the gas bubbles, while the other is for liquid plugs. Due to the limited experimental conditions and not having videos of the flow for comparison, it was not possible to generalize the efficacy of the method to other flow patterns.

5. ACKNOWLEDGEMENTS

This study was financed in part by the Coordenação de Aperfeiçoamento de Pessoal de Nível Superior – Brasil (CAPES) – Finance Code 001.

Fundação de Amparo à Pesquisa do Estado de São Paulo (FAPESP).

6. REFERENCES

Berto, A., Lavieille, P., Azzolin, M., Bortolin, S., Miscevic, M. and Col, D.D., 2021. "Liquid film thickness and heat transfer measurements during downflow condensation inside a small diameter tube". *International Journal of Multiphase Flow*, Vol. 140, p. 103649. doi:10.1016/j.ijmultiphaseflow.2021.103649.

Chen, L., Tian, Y. and Karayiannis, T., 2006. "The effect of tube diameter on vertical two-phase flow regimes in small tubes". *International Journal of Heat and Mass Transfer*, Vol. 49, No. 21-22, pp. 4220–4230. doi:10.1016/j.ijheatmasstransfer.2006.03.025.

Cioncolini, A. and Thome, J.R., 2013. "Liquid film circumferential asymmetry prediction in horizontal annular two-phase flow". *International Journal of Multiphase Flow*, Vol. 51, pp. 44–54. doi:10.1016/j.ijmultiphaseflow.2012.12.003.

Coleman, J.W. and Garimella, S., 1999. "Characterization of two-phase flow patterns in small diameter round and rectangular tubes". *International Journal of Heat and Mass Transfer*, Vol. 42, No. 15, pp. 2869–2881. doi:10.1016/s0017-9310(98)00362-7.

Mandhane, J., Gregory, G. and Aziz, K., 1974. "A flow pattern map for gas—liquid flow in horizontal pipes". *International Journal of Multiphase Flow*, Vol. 1, No. 4, pp. 537–553. doi:10.1016/0301-9322(74)90006-8.

Revellin, R., Dupont, V., Ursenbacher, T., Thome, J.R. and Zun, I., 2006. "Characterization of diabatic two-phase flows in microchannels: Flow parameter results for r-134a in a 0.5mm channel". *International Journal of Multiphase Flow*, Vol. 32, No. 7, pp. 755–774. doi:10.1016/j.ijmultiphaseflow.2006.02.016.

Seo, J., Lee, S., Yang, S.R. and Hassan, Y.A., 2021. "Experimental investigation of the annular flow caused by convective boiling in a heated annular channel". *Nuclear Engineering and Design*, Vol. 376, p. 111088. doi:10.1016/j.nucengdes.2021.111088.

Taitel, Y. and Dukler, A.E., 1976. "A model for predicting flow regime transitions in horizontal and near horizontal gas-liquid flow". *AIChE Journal*, Vol. 22, No. 1, pp. 47–55. doi:10.1002/aic.690220105.

Thome, J., Bar-Cohen, A., Revellin, R. and Zun, I., 2013. "Unified mechanistic multiscale mapping of two-phase flow patterns in microchannels". *Experimental Thermal and Fluid Science*, Vol. 44, pp. 1–22. doi:10.1016/j.expthermflusci.2012.09.012.

Tibiriçá, C.B., do Nascimento, F.J. and Ribatski, G., 2010. "Film thickness measurement techniques applied to micro-scale two-phase flow systems". *Experimental Thermal and Fluid Science*, Vol. 34, No. 4, pp. 463–473. doi:10.1016/j.expthermflusci.2009.03.009.

Triplett, K., Ghiaasiaan, S., Abdel-Khalik, S., LeMouel, A. and McCord, B., 1999. "Gas–liquid two-phase flow in microchannels". *International Journal of Multiphase Flow*, Vol. 25, No. 3, pp. 395–410. doi:10.1016/s0301-9322(98)00055-x.

Wambsganss, M., Jendrzejczyk, J. and France, D., 1991. "Two-phase flow patterns and transitions in a small, horizontal, rectangular channel". *International Journal of Multiphase Flow*, Vol. 17, No. 3, pp. 327–342. doi:10.1016/0301-9322(91)90003-l.

Wojtan, L., Ursenbacher, T. and Thome, J.R., 2005. "Investigation of flow boiling in horizontal tubes: Part i—a new diabatic two-phase flow pattern map". *International Journal of Heat and Mass Transfer*, Vol. 48, No. 14, pp. 2955–2969. doi:10.1016/j.ijheatmasstransfer.2004.12.012.

Zaitsev, D., Kochkin, D. and Kabov, O., 2022. "Dynamics of liquid film rupture under local heating". *International Journal of Heat and Mass Transfer*, Vol. 184, p. 122376. doi:10.1016/j.ijheatmasstransfer.2021.122376.

7. RESPONSIBILITY NOTICE

The authors are solely responsible for the printed material included in this paper.